HHS Public Access

Author manuscript

Genesis. Author manuscript; available in PMC 2019 August 10.

Published in final edited form as:

Genesis. 2018 August ; 56(8): e23223. doi:10.1002/dvg.23223.

A mouse model engineered to conditionally express the progesterone receptor-B isoform

Lan Hai[1,#], **Maria M. Szwarc**[1,#], **Margeaux Wetendorf**[2,#], **San-Pin Wu**[3], **Mary C. Peavey**[4], **Sandra L. Grimm**[1], **Dean P. Edwards**[1], **Francesco J. DeMayo**[3], and **John P. Lydon**[1]

[1]Department of Molecular & Cellular Biology, Baylor College of Medicine, One Baylor Plaza, Houston, Texas, 77030;

[2]University of North Carolina Chapel Hill, Chapel Hill, NC 27599;

[3]Reproductive and Developmental Biology Laboratory, National Institute of Environmental Health Sciences, Research Triangle Park, North Carolina, 27709;

[4]UNC Fertility, Raleigh, NC 27617.

Abstract

Using a *Rosa26* gene targeting strategy in mouse embryonic stem cells, we have generated a new transgenic mouse (*Pgr-B*^{LSL}), which is designed to conditionally express the epitope-tagged mouse progesterone receptor-B (PGR-B) isoform when crossed with a specific cre driver mouse. To functionally validate this transgenic mouse, we crossed the *Pgr-B*^{LSL} mouse with the *MMTV-CREA* transgenic mouse to create the *MMTV-CREA/Pgr-B*^{LSL} bigenic (termed PR-B:OE to denote PGR-B overexpressor). As expected, transgene-derived PGR-B protein was specifically targeted to the virgin mammary gland epithelium. At a functional level, the PR-B:OE bigenic exhibited abnormal mammary morphogenesis—dilated epithelial ducts, precocious alveologenesis and lateral side-branching, along with a prominent proliferative signature—that resulted in pregnant PR-B:OE mice unable to exhibit mammary gland terminal differentiation at parturition. Because of this developmental failure, the PR-B:OE mammary gland was incapable of producing milk resulting in early neonatal death of otherwise healthy litters. This first line of analysis demonstrates the utility of the *Pgr-B*^{LSL} mouse to examine the role of the PGR-B isoform in different physiologic and pathophysiologic systems that are responsive to progesterone.

Keywords

Transgenic; Mouse; Progesterone Receptor-B; Isoform; Mammary Gland; Proliferation; Differentiation; Lactation

Correspondence to: Francesco J. DeMayo; John P. Lydon.

[#]Co-primary authors. **Correspondence to:** John P. Lydon, Ph.D., Department of Molecular & Cellular Biology, M732A, Baylor College of Medicine, One Baylor Plaza, Houston,, Texas, 77030, USA., Telephone: (713) 798-3534, Telefax: (713) 797-1275, jlydon@bcm.edu.

1 INTRODUCTION

The progesterone receptor (PGR) transduces the progesterone hormone signal into a transcriptional response that drives essential molecular and cellular changes for normal development and function of the female reproductive tract and mammary gland (Fernandez-Valdivia *et al.*, 2005; Grimm *et al.*, 2016; Scarpin *et al.*, 2009). As a member of the nuclear receptor superfamily of transcription factors, the PGR comprises two isoforms: PGR-A and PGR-B (Giangrande and McDonnell, 1999). Expressed from the same gene by two different promoters, the PGR-A and PGR-B isoforms share an identical amino acid sequence but vary by a 165 amino acid extension at the N-terminus of the PGR-B isoform (Bain *et al.*, 2001; Takimoto *et al.*, 2003; Vegeto *et al.*, 1993). *In vitro* studies were the first to indicate that the PGR-A and PGR-B isoforms exhibit different transactivational properties (Conneely and Lydon, 2000; Giangrande and McDonnell, 1999; Richer *et al.*, 2002; Vegeto *et al.*, 1993), suggesting that these receptor isotypes may exert different functional roles *in vivo*.

We have used experimental mouse genetics to functionally abrogate both PGR isoforms simultaneously or each isoform separately (Lydon *et al.*, 1995; Mulac-Jericevic *et al.*, 2003; Mulac-Jericevic *et al.*, 2000). We have also taken advantage of the murine *Pgr* allele to knockin the lacZ reporter gene (Ismail *et al.*, 2002), the cre recombinase gene (Mukherjee *et al.*, 2006; Soyal *et al.*, 2005), the reverse tetracycline transactivator gene (Mukherjee *et al.*, 2007), and select point mutations (Grimm *et al.*, 2014). Further genetic manipulations include the generation of mice harboring a *Pgr* conditional knockout (or floxed) allele (Fernandez-Valdivia *et al.*, 2010).

Selective ablation of the PGR-A or PGR-B isoforms in the mouse confirmed the predicted selective functional roles of these nuclear receptor isoforms *in vivo* (Mulac-Jericevic *et al.*, 2003; Mulac-Jericevic *et al.*, 2000). Molecular, cellular, and physiological studies revealed that the PGR-A isoform is critical for progesterone responses that underpin normal uterine and ovarian function whereas the PGR-B isoform was shown to mediate the majority of mammary morphogenetic changes that occur with early parity when serum progesterone levels are high. Specifically, absence of the PGR-B isoform in the PGR-B knockout mouse resulted in a marked reduction in mammary gland epithelial side-branching and alveologenesis due to a significant attenuated proliferative response to progesterone.

Apart from a knockout approach to disrupt the normal stoichiometry of the PGR-A and PGR-B isoforms, we recently used advanced transgenic approaches to generate a mouse model in which the expression levels of the PGR-A isoform are significantly elevated (Wetendorf *et al.*, 2017). This transgenic approach demonstrated a pivotal role for this receptor isotype in controlling the window of receptivity in the mouse uterus. Using an identical genetic strategy, we report here the design, generation, and first-line characterization of a new transgenic mouse (termed the *Pgr-B*^{LSL} mouse), which is engineered to conditionally express the murine PGR-B isoform when crossed with the appropriate cre driver mouse.

2 RESULTS AND DISCUSSION

2.1 Generation of the *Pgr-B*^{LSL} transgenic mouse

Before generating the *Pgr-B*^{LSL} transgenic mouse, we confirmed that the epitope-tagged murine PGR-B isoform exhibits significant transactivational activity in response to progesterone *in vitro* (Supporting Information Figure 1). Using our established gene targeting strategy to knockin minigenes by homologous recombination into the *Rosa26* locus of mouse ES cells (Szwarc *et al.*, 2014; Wetendorf *et al.*, 2017; Wu *et al.*, 2010), we targeted a minigene carrying a powerful ubiquitous promoter (*CAGGSp*), a Lox-STOP-Lox (LSL) cassette followed by a cDNA encoding the epitope-tagged murine PGR-B isoform (Figure 1a). In the presence of cre recombinase, the STOP signal is excised to allow *CAGGSp* promoter-driven expression of the *Pgr-B* cDNA in tissues specified by the promoter that drives cre expression. Using this targeting strategy, we achieved an efficient targeting frequency of approximately 20% (5/24) as shown by Southern analysis (Figure 1b), without the need for negative selection. With previous reported methods (Lydon *et al.*, 1995), three independent mouse lines were established using ES cell clones: #4, #10, and #17. To functionally validate #4, #10, and #17 mouse lines carrying the *Pgr-B*^{LSL} minigene, the three separate lines were crossed with the MMTV-CREA transgenic mouse to generate the PR-B:OE bigenic (Figure 1c), which is predicted to target cre expression and activity mostly to the mammary gland epithelium (Wagner *et al.*, 1997). Initial analysis demonstrated that the three mouse lines operated as designed (data not shown); *Pgr-B*^{LSL} mice derived from ES clone #17 were used further in this study. Western immunoblot analysis confirmed that the PR-B:OE mouse expresses the transgene-derived epitope-tagged PGR-B isoform in the mammary gland epithelium (Figure 1d). Note: In the normal adult virgin mammary gland, expression of the PGR-A isoform predominates (Aupperlee *et al.*, 2005).

2.2 The adult virgin PR-B:OE mouse targets epitope-tagged PR-B isoform expression to the mammary epithelium

For consistency, both control and PR-B:OE mice were examined at the progesterone-dominant diestrus phase of their estrous cycle (Figure 2a, b). Immunohistochemical analysis confirmed that the epitope-tagged PGR-B isoform is expressed in the majority of cells in the mammary epithelial compartment of the PR-B:OE adult virgin mouse (Figure 2 c-f). Interestingly, the PR-B:OE mammary gland consistently displayed an increased number of mammary epithelial cells that scored positive for BrdU. This result supports the known mitogenic role of progesterone hormone in the murine mammary gland (Fernandez-Valdivia *et al.*, 2005). Compared to control siblings, whole mount analysis revealed that the PR-B:OE mouse exhibited a more complex ductal architecture in their mammary glands, which manifested as increased ductal side-branching and nascent alveolar budding (Figure 3). Although not as conspicuous, the diameter of the PR-B:OE mammary epithelial ducts appeared larger than their control counterparts. However, this ductal dilation with pronounced epithelial proliferation in the PR-B:OE mammary gland becomes more obvious with age (Support Information Figure S2). Interestingly, this morphological response is also accompanied by a striking increase in the expression levels of the cytokine RANKL (Support Information Figure S2), a known target of the PGR-B isoform in the murine mammary gland (Mulac-Jericevic *et al.*, 2003; Obr *et al.*, 2013).

2.3 Overexpression of the PGR-B isoform blocks mammary gland differentiation at parturition

To assess whether PR-B:OE dams can produce and maintain viable litters, PR-B:OE females were mated with CD1 proven stud males to generate monogenic control litters. Although the PR-B:OE female is fertile and produces normal litter sizes at parturition, pups from these dams die soon after birth (Figure 4a). Examination of 48 hour old pups from control and PR-B:OE dams revealed milk in the stomach of pups from control dams but an absence of milk in the stomach of pups from PR-B:OE dams (Figure 4b and c). However, PR-B:OE dams exhibit normal maternal behavior, and pups from these dams attempt to suckle (data not shown). Moreover, fostering experiments demonstrate that 24-hour old monogenic control pups from PR-B:OE dams can be rescued by fostering with synchronized parturient CD1 dams (three litters from three separate PR-B:OE dams (litter 1 (n=7 pups); litter 2 (n=9 pups); and litter 3 (n= 8 pups)). Together, these findings indicate that the PR-B:OE mammary gland fails to synthesize and/or secrete milk at lactation.

Whole mount analysis shows that the control mammary gland develops into a typical lactating mammary gland, with an extensive lobuloalveolar epithelial network that occupies most of the fat pad (Figure 5a). Conversely, the PR-B:OE mammary gland displays overt dilated ducts with abnormal alveolar budding (Figure 5b). Unlike the control mammary gland at lactation, the PR-B:OE mammary gland epithelium does not show signs of terminal differentiation as evidenced by the absence of lipid droplets in mammary epithelial cells (compare Figure 5c with d). Higher magnification clearly shows the marked absence of vacuolated lipid droplets in the PR-B:OE mammary gland epithelial compartment (compare Figure 5e with f). Histochemical analysis shows that most of the PR-B:OE mammary gland at this developmental stage is composed of dilated epithelial ducts with abnormal alveolar buds (Figure 5g) and areas with foci of proliferating mammary epithelial cells (Figure 5h). Immunohistochemical analysis also shows that the PR-B:OE mammary continues to express high levels of the epitope-tagged PGR-B isoform whereas PGR expression is absent in the control gland at this time (Supporting Information Figure S3). The abnormal mitogenic response of the PR-B:OE mammary gland is also reflected at the molecular level with increased transcript levels of PGR mammary targets that are involved in mammary epithelial proliferation (*i.e. Ccnd1* (cyclin D1), *Tnfsf11* (RANKL), and *Wnt4* (Fernandez-Valdivia *et al.*, 2008)) and a significant reduction in gene expression associated with mammary gland differentiation at parturition (*i.e. Csn2* (casein) and *Wap (whey acidic protein)*) (Figure 6).

2.4 Utility of the *Pgr-B^{LSL}* transgenic mouse

Our initial characterization of the *Pgr-B^{LSL}* transgenic mouse underscores the utility of this new transgenic mouse to interrogate the role of the PGR-B isoform in physiological and pathological systems that are responsive to progesterone exposure. Because of the availability of suitable cre driver mice (Regan *et al.*, 2000; Soyal *et al.*, 2005; Wagner *et al.*, 1997), immediate applications of the *Pgr-B^{LSL}* mouse include assessing the functional role of the PGR-B isoform in: (a) myometrial contractility at parturition (Tan *et al.*, 2012); (b) the pathogenesis of uterine leiomyomas (Bulun *et al.*, 2015; Patel *et al.*, 2015; Tsigkou *et al.*, 2015); and (c) early mammary gland metastasis (Hosseini *et al.*, 2016). As with the majority of transgenic mouse models, caution needs to be taken when interpreting the phenotypes

displayed by the PR-B:OE mouse as the levels of PGR-B expressed by this transgenic are significantly higher than the levels of endogenous PGR-B.

Nearly two decades ago, two transgenic mouse models were reported to express the PGR-A and PGR-B isoforms (Chou *et al.*, 2003; Fleisch *et al.*, 2009; Shyamala *et al.*, 2000; Shyamala *et al.*, 1998). However, these bi-transgenic mice exhibit inherent weaknesses, such as (a) reliance on the yeast GAL-4 transcription factor to drive (in trans) expression of the transgene, which undermines its wider applicability; (b) the CMV promoter used in this transgenic design results in global rather than targeted expression of the transgene; (c) lack of epitope-tags so that the transgene-derived PGR isoform cannot be differentiated from the corresponding endogenous receptor; and (d) absence of western data to confirm that the PGR isoform protein was expressed from the transgene. In contrast, we provide a detailed characterization of a new PGR-B transgenic mouse which is designed for wide applicability to study the role of this PGR isoform in a number of progesterone target tissues *in vivo*.

3 MATERIALS AND METHODS

3.1 Establishment of the *Pgr-B^{LSL}* transgenic mouse

The basic generic design and general recombineering strategy to generate the targeting vector has been described (Wetendorf *et al.*, 2017; Wu *et al.*, 2010). Briefly, the targeting vector contains 5' and 3' arms of *Rosa26* genomic sequences, which are required for homologous recombination with equivalent sequences within the *Rosa26* locus of mouse ES cells (Wetendorf *et al.*, 2017; Wu *et al.*, 2010). The 5' and 3' arms flank a minigene, which consists of (in the 5' to 3' direction): the *CAGGS* promoter; a *LoxP-STOP-LoxP* (LSL) cassette; a cDNA encoding the epitope-tagged mouse PGR-B isoform; and a polyadenylation signal. The constitutively active *CAGGS* composite promoter comprises the chicken β-actin promoter and the cytomegalovirus (CMV) enhancer. The FLAG-Myc epitope tag is fused in-frame to the 5' end of the PGR-B isoform; the 3' rabbit globin polyadenylation signal acts as a strong polyadenylation signal for the minigene. The targeting vector also contains the diphtheria toxin A (DTA) gene for negative selection (located 3' to the 3' *Rosa26* homology arm of the targeting vector); however, negative selection was not required in these studies due to the high targeting efficiency at the *Rosa26* locus. The linearized targeting vector (25ug) was electroporated into mouse AB2.2 ES cells as previously described (Wetendorf *et al.*, 2017; Wu *et al.*, 2010). Targeted ES clones were identified by Southern analysis of their EcoRV digested genomic DNA. Positive ES clones, which were heterozygous for the targeted event, were scored by the presence of both 11.5kb and 3.8kb hybridization bands corresponding to the wild-type and targeted *Rosa26* alleles respectively. Standard procedures were used to generate chimeric founder (F0) mice from targeted ES clones (Szwarc *et al.*, 2014; Wetendorf *et al.*, 2017; Wu *et al.*, 2010). At least three individual targeted ES clones were used to generate separate monogenic *Pgr-B^{LSL}* mouse lines, each of which harbored a single copy of the minigene. With this minigene design, cell-type specific expression of the epitope-tagged PGR-B (driven by the *CAGGS* promoter) is achieved by excision of the interposed LSL cassette by a cre recombinase controlled by a specific promoter. Upon request, the *Pgr-B^{LSL}* transgenic mouse will be made available to the research community.

3.2 Creation of the *MMTV-CREA: Pgr-B^{LSL}* (PR-B:OE) bigenic mouse

To test the efficacy of the *Pgr-B^{LSL}* mouse to conditionally overexpress the epitope-tagged PGR-B isoform when crossed with a cre-driver mouse, the mouse mammary tumor virus (*MMTV)-CREA* transgenic mouse (Wagner *et al.*, 1997) was crossed with a number of *Pgr-B^{LSL}* lines to generate the bigenic *MMTV-CREA: Pgr-B^{LSL}* mouse. Resultant *MMTV-CREA: Pgr-B^{LSL}* bigenic mice were maintained in a mixed 129SvEv/C57BL6 background and referred to as PR-B overexpressor (PR-B:OE) mice. Mice were genotyped by Southern and PCR methods as previously described (Szwarc *et al.*, 2014; Wetendorf *et al.*, 2017; Wu *et al.*, 2010).

Mouse housing and husbandry was conducted in an AAALAC accredited *vivarium* in Baylor College of Medicine. Within temperature regulated rooms (22 ± 2^{o}C) with a light-dark photocycle, mice were provided irradiated global soy protein-free extruded rodent chow (Harlan Laboratories, Inc. Indianapolis, IN) and fresh water *ad libitum*. Animal studies were undertaken in accordance with the guidelines detailed in the Guide for the Care and Use of Laboratory Animals ("The Guide" (Eighth Edition 2011)), which is published by the National Research Council of the National Academies, Washington, D.C. (www.nap.edu). Animal protocols followed in these investigations were prospectively approved by the Institutional Animal Care and Use Committee (IACUC) at Baylor College of Medicine.

3.3 Timed pregnancies, fostering and staging the estrous cycle

For timed pregnancies and lactation, control and PR-B:OE females (9–10 weeks old) were housed with proven stud/breeder C57BL/6 males overnight. Detection of the vaginal plug the following morning was designated as gestation day 1 (GD 1). Pregnant females were individually housed before euthanasia on a specified day of pregnancy or lactation. The number of viable or nonviable pups per litter following birth was recorded for both control and PR-B:OE dams. For fostering of litters from PR-B:OE dams, proven stud CD1 males were first mated with sexually mature PR-B:OE females to produce monogenic control pups. Twenty-four hours after birth, PR-B:OE dams and peri-parturient synchronized CD1 foster dams were removed from their cages and placed in separate clean cages. Following removal of the CD1 foster dam's litter, the litter of the PR-B:OE dam was transferred gently into the CD1 foster dam's cage, where the litter was mixed with dirty bedding and nesting material from the CD1 foster mother to transfer the CD1 foster dam's scent. The CD1 foster mother was then returned to its cage with the PR-B:OE litter. Following return of the CD1 foster dam, the PR-B:OE litter was monitored every 15 minutes for the first three-hours. To decrease the chance of cannibalism, the foster litter was not disturbed for 72 hours after fostering. After the first 72 hours, the cages were observed daily until the foster pups were weaned. To evaluate estrous cycle progression, mice were monitored daily for 3–4 weeks by examining the cytology of vaginal lavages on glass slides, which were stained with 10% crystal violet (Sigma-Aldrich, St. Louis, MO) using an established protocol (Hai *et al.*, 2018). For these studies, virgin mice at diestrus were examined.

3.4 Mammary gland whole-mount and immunohistochemistry

Using established methods (Mukherjee *et al.*, 2010), inguinal (#4) mammary glands (carefully spread on glass slides) were fixed in an ethanol: acetic acid (3:1) mixture

overnight before rehydration the next day with 70% ethanol and subsequently water. Hydrated and fixed mammary tissues were then stained with carmine aluminum stain overnight. The following morning, mammary gland fat pads were clarified with toluene for at least 24–48 hours prior to mounting coverslips with permount (ThermoFisher Scientific Inc., Waltham, MA).

For immunohistochemical analysis, mammary gland tissues were fixed in 4% paraformaldehyde (PFA) overnight before being processed and embedded in paraffin as previously reported (Mukherjee *et al.*, 2010). From paraffin-embedded mammary tissue blocks, tissue sections (5μm) were placed on Superfrost plus glass slides (ThermoFisher Scientific Inc.). Tissue sections were deparaffinized, rehydrated, and processed through an antigen unmasking step before immunohistochemical staining. After a 1-hour blocking step at room temperature, tissue sections were incubated with the appropriate primary antibody overnight at 4^{o}C as previously described (Mukherjee *et al.*, 2011; Szwarc *et al.*, 2014; Szwarc *et al.*, 2017). The following antibodies were used in these studies: a rabbit anti-Myc-epitope tagged 71D10 monoclonal antibody (Cell Signaling Technology, Danvers, MA (1/200; #2278)) and a rabbit polyclonal anti- human PGR antibody (Santa Cruz Biotechnology, Dallas, TX (1/300; #sc7208)). Following incubation with the primary antibody, mammary tissue sections were incubated with an anti-rabbit IgG secondary antibody (Vector laboratories, Inc., Burlingame, CA) for 1 hour at room temperature. Sections were then incubated with the R.T.U. Vectastain® Universal ABC reagent (Vector laboratories, Inc.) for 30 minutes at room temperature. A positive immunoreaction *in situ* was visualized by incubating with 3, 3'-diaminobenzidine ((DAB) Vector laboratories Inc.) before sections were counterstained with hematoxylin. Tissue sections were dehydrated before glass coverslips were affixed using permount (ThermoFisher Scientific Inc. (#SP15–500)). To immunohistochemically detect 5'-bromo-2'-deoxyuridine (BrdU) incorporation in mammary tissue, mice were intraperitoneally (I.P.) injected with BrdU (10mg/ml; Amersham Biosciences Corporation, Piscataway, NJ (0.1ml/10g body weight)) two hours prior to euthanasia. After tissue processing as detailed above, mammary tissue sections were incubated overnight at room temperature with a biotinylated anti-BrdU antibody (BrdU In-Situ Detection Kit (BD Pharmingen Inc., San Jose, CA; 1:10 dilution)). Mammary tissue sections were then incubated with the Vectastain ABC reagent at room temperature for 1 hour; immunopositivity was detected using the DAB peroxidase substrate kit. Our previously published protocol and antibodies for immunofluorescence detection of RANKL expression in the mammary epithelium was followed in these studies (Fernandez-Valdivia *et al.*, 2009; Mukherjee *et al.*, 2010).

Images of immunostained mammary tissue sections were captured using a color-chilled AxioCam MRc5 digital camera connected to a Carl Zeiss AxioImager A1 upright microscope (Zeiss, Jena, Germany). Post image processing and annotation were performed using Adobe Photoshop® and Illustrator® (CS6 version) software programs (Adobe Systems Inc., San Jose, CA).

3.5 Molecular studies

Isolation of mammary epithelial cells for starting material for quantitative real time PCR and western analysis has been described (Mukherjee *et al.*, 2010). For quantitative real-time PCR, total RNA was extracted from isolated mammary epithelial cells using TRIzol® reagent (ThermoFisher Scientific Inc.) and further purified using the RNeasy® Plus Mini Kit (Qiagen Inc., Germantown Road, MD). Reverse transcription of total RNA into cDNA was conducted with the Superscript™ IV VILO™ Master Mix (ThermoFisher Scientific Inc) prior to real-time PCR amplification. Detailed information concerning the TaqMan® gene expression assays used in these experiments is described in Supporting Information Table S1; the 18S ribosomal RNA TaqMan® assay represented the internal control.

Western immunoblotting conditions have been reported previously (Hai *et al.*, 2018; Mukherjee *et al.*, 2010). The following primary antibodies (all at 1/1000 dilution) used in these investigations are: a monoclonal anti-FLAG® M2 antibody (Sigma-Aldrich; #F3165); a rabbit anti-Myc-epitope tagged 71D10 monoclonal antibody (Cell Signaling Technology; #2278); and a rabbit polyclonal anti-PGR antibody (Santa Cruz Biotechnology Inc.; #sc7208). The SuperSignal™ West Pico Chemiluminescent Substrate kit (ThermoFisher Scientific Inc.) detected the chemiluminescent signal. Re-probing of western blots with different antibodies was achieved by using Restore Western Blot Stripping buffer (ThermoFisher Scientific Inc.).

3.6 *In vitro* transient transfection assay

To assess the *in vitro* transactivational activity of the epitope-tagged murine PGR-B isoform that was used to make the transgenic mouse, HeLa cells were plated on 6-well plates ($1X10^5$ cells per well) in Dulbecco's Modified Eagle's Medium ((DMEM) ThermoFisher Scientific Inc.) with 10% fetal bovine serum ((FBS) Sigma-Aldrich, St. Louis, MO). After 48 hours of culture, cells were refed with DMEM without phenol red (DMEM w/o; ThermoFisher Scientific Inc.) with 2% charcoal-stripped (s) FBS (Sigma-Aldrich) before transfecting with a luciferase reporter (3μg per well) containing tandem progesterone response elements (PRE_2) and a TATA box located on the 5' end of the Renilla Luciferase reporter gene (PRE_2-TATA-Luc) (Wardell *et al.*, 2002). The reporter plasmid was co-transfected with a lentivirus expression vector ((pLenti (3 μg per well)) Origene Inc., Rockville MD) expressing the epitope-tagged murine PGR protein (pLenti-Pgr) or the control empty vector. To normalize transfection efficiency, the Renilla Luciferase control reporter vector DNA ((pTK-RL (300ng per well)) Promega, Madison, WI) was included with each transfection. The FuGENE® HD Transfection Reagent (Promega (9ul per well)) was used for DNA delivery; FuGENE-DNA complexes were formed according to the manufacturer's instructions. Twenty-four hours post-transfection, cells were plated in 96-well white optical bottom plates at $2X10^4$ cells per well in DMEM w/o with 2% sFBS. After allowing 24 hours for cell attachment, cells were treated with either $5X10^{-6}$ M medroxyprogesterone acetate (MPA; Sigma Aldrich) or vehicle control for 24 hours. Luciferase activity was measured using the Dual-Glo® kit (Promega) according to the manufacturer's instructions.

3.7 Statistical analysis

As required, two-tailed student's t tests or two-way ANOVA with *post-hoc* Tukey's range test were conducted with the GraphPad Prism and Instat tools (GraphPad software Inc., La Jolla, CA). Statistical significance was indicated by a p-value of <0.05; asterisks in bar graphs denote the level of significance: *p<0.05; **P<0.01; and ***p<0.001.

Supplementary Material

Refer to Web version on PubMed Central for supplementary material.

ACKNOWLEDGMENTS

We thank Jie Li, Yan Ying, and Rong Zhao for their technical expertise. The technical support of the Mouse Embryonic Stem Cell and Genetically Engineered Mouse cores at Baylor College of Medicine are gratefully acknowledged. We thank Dr. Michael T. Lewis, Breast Center at Baylor College of Medicine, for providing the MMTV-CREA transgenic mouse. This research was supported in part by the National Institutes of Health (NIH)/ National Institute of Child Health and Human Development (NICHD) grant: HD-042311 to JPL.

REFERENCES

Aupperlee MD, Smith KT, Kariagina A, Haslam SZ. 2005 Progesterone receptor isoforms A and B: temporal and spatial differences in expression during murine mammary gland development. Endocrinology 146: 3577–3588. [PubMed: 15878961]

Bain DL, Franden MA, McManaman JL, Takimoto GS, Horwitz KB. 2001 The N-terminal region of human progesterone B-receptors: biophysical and biochemical comparison to A-receptors. J Biol Chem 276: 23825–23831. [PubMed: 11328821]

Bulun SE, Moravek MB, Yin P, Ono M, Coon JSt, Dyson MT, Navarro A, Marsh EE, Zhao H, Maruyama T, Chakravarti D, Kim JJ, Wei JJ. 2015 Uterine Leiomyoma Stem Cells: Linking Progesterone to Growth. Semin Reprod Med 33: 357–365. [PubMed: 26251118]

Chou YC, Uehara N, Lowry JR, Shyamala G. 2003 Mammary epithelial cells of PR-A transgenic mice exhibit distinct alterations in gene expression and growth potential associated with transformation. Carcinogenesis 24: 403–409. [PubMed: 12663498]

Conneely OM, Lydon JP. 2000 Progesterone receptors in reproduction: functional impact of the A and B isoforms. Steroids 65: 571–577. [PubMed: 11108861]

Fernandez-Valdivia R, Jeong J, Mukherjee A, Soyal SM, Li J, Ying Y, Demayo FJ, Lydon JP. 2010 A mouse model to dissect progesterone signaling in the female reproductive tract and mammary gland. Genesis 48: 106–113. [PubMed: 20029965]

Fernandez-Valdivia R, Mukherjee A, Creighton CJ, Buser AC, DeMayo FJ, Edwards DP, Lydon JP. 2008 Transcriptional response of the murine mammary gland to acute progesterone exposure. Endocrinology 149: 6236–6250. [PubMed: 18687774]

Fernandez-Valdivia R, Mukherjee A, Mulac-Jericevic B, Conneely OM, DeMayo FJ, Amato P, Lydon JP. 2005 Revealing progesterone's role in uterine and mammary gland biology: insights from the mouse. Semin Reprod Med 23: 22–37. [PubMed: 15714387]

Fernandez-Valdivia R, Mukherjee A, Ying Y, Li J, Paquet M, DeMayo FJ, Lydon JP. 2009 The RANKL signaling axis is sufficient to elicit ductal side-branching and alveologenesis in the mammary gland of the virgin mouse. Dev Biol 328: 127–139. [PubMed: 19298785]

Fleisch MC, Chou YC, Cardiff RD, Asaithambi A, Shyamala G. 2009 Overexpression of progesterone receptor A isoform in mice leads to endometrial hyperproliferation, hyperplasia and atypia. Mol Hum Reprod 15: 241–249. [PubMed: 19224949]

Giangrande PH, McDonnell DP. 1999 The A and B isoforms of the human progesterone receptor: two functionally different transcription factors encoded by a single gene. Recent Prog Horm Res 54: 291–313; discussion 313–294. [PubMed: 10548881]

Grimm SL, Hartig SM, Edwards DP. 2016 Progesterone Receptor Signaling Mechanisms. J Mol Biol 428: 3831–3849. [PubMed: 27380738]

Grimm SL, Ward RD, Obr AE, Franco HL, Fernandez-Valdivia R, Kim JS, Roberts JM, Jeong JW, DeMayo FJ, Lydon JP, Edwards DP, Weigel NL. 2014 A role for site-specific phosphorylation of mouse progesterone receptor at serine 191 in vivo. Mol Endocrinol 28: 2025–2037. [PubMed: 25333515]

Hai L, Szwarc MM, He B, Lonard DM, Kommagani R, DeMayo FJ, Lydon JP. 2018 Uterine function in the mouse requires speckle-type poz protein. Biol Reprod.

Hosseini H, Obradovic MM, Hoffmann M, Harper KL, Sosa MS, Werner-Klein M, Nanduri LK, Werno C, Ehrl C, Maneck M, Patwary N, Haunschild G, Guzvic M, Reimelt C, Grauvogl M, Eichner N, Weber F, Hartkopf AD, Taran FA, Brucker SY, Fehm T, Rack B, Buchholz S, Spang R, Meister G, Aguirre-Ghiso JA, Klein CA. 2016 Early dissemination seeds metastasis in breast cancer. Nature.

Ismail PM, Li J, DeMayo FJ, O'Malley BW, Lydon JP. 2002 A novel LacZ reporter mouse reveals complex regulation of the progesterone receptor promoter during mammary gland development. Mol Endocrinol 16: 2475–2489. [PubMed: 12403837]

Lydon JP, DeMayo FJ, Funk CR, Mani SK, Hughes AR, Montgomery CA, Jr, Shyamala G, Conneely OM, O'Malley BW. 1995 Mice lacking progesterone receptor exhibit pleiotropic reproductive abnormalities. Genes Dev 9: 2266–2278. [PubMed: 7557380]

Mukherjee A, Soyal SM, Fernandez-Valdivia R, DeMayo FJ, Lydon JP. 2007 Targeting reverse tetracycline-dependent transactivator to murine mammary epithelial cells that express the progesterone receptor. Genesis 45: 639–646. [PubMed: 17941046]

Mukherjee A, Soyal SM, Li J, Ying Y, He B, DeMayo FJ, Lydon JP. 2010 Targeting RANKL to a specific subset of murine mammary epithelial cells induces ordered branching morphogenesis and alveologenesis in the absence of progesterone receptor expression. FASEB J 24: 4408–4419. [PubMed: 20605949]

Mukherjee A, Soyal SM, Li J, Ying Y, Szwarc MM, He B, Kommagani R, Hodgson MC, Hiremath M, Cowin P, Lydon JP. 2011 A mouse transgenic approach to induce beta-catenin signaling in a temporally controlled manner. Transgenic Res 20: 827–840. [PubMed: 21120693]

Mukherjee A, Soyal SM, Wheeler DA, Fernandez-Valdivia R, Nguyen J, DeMayo FJ, Lydon JP. 2006 Targeting iCre expression to murine progesterone receptor cell-lineages using bacterial artificial chromosome transgenesis. Genesis 44: 601–610. [PubMed: 17149722]

Mulac-Jericevic B, Lydon JP, DeMayo FJ, Conneely OM. 2003 Defective mammary gland morphogenesis in mice lacking the progesterone receptor B isoform. Proc Natl Acad Sci U S A 100: 9744–9749. [PubMed: 12897242]

Mulac-Jericevic B, Mullinax RA, DeMayo FJ, Lydon JP, Conneely OM. 2000 Subgroup of reproductive functions of progesterone mediated by progesterone receptor-B isoform. Science 289: 1751–1754. [PubMed: 10976068]

Obr AE, Grimm SL, Bishop KA, Pike JW, Lydon JP, Edwards DP. 2013 Progesterone receptor and Stat5 signaling cross talk through RANKL in mammary epithelial cells. Mol Endocrinol 27: 1808–1824. [PubMed: 24014651]

Patel B, Elguero S, Thakore S, Dahoud W, Bedaiwy M, Mesiano S. 2015 Role of nuclear progesterone receptor isoforms in uterine pathophysiology. Hum Reprod Update 21: 155–173. [PubMed: 25406186]

Regan CP, Manabe I, Owens GK. 2000 Development of a smooth muscle-targeted cre recombinase mouse reveals novel insights regarding smooth muscle myosin heavy chain promoter regulation. Circ Res 87: 363–369. [PubMed: 10969033]

Richer JK, Jacobsen BM, Manning NG, Abel MG, Wolf DM, Horwitz KB. 2002 Differential gene regulation by the two progesterone receptor isoforms in human breast cancer cells. J Biol Chem 277: 5209–5218. [PubMed: 11717311]

Scarpin KM, Graham JD, Mote PA, Clarke CL. 2009 Progesterone action in human tissues: regulation by progesterone receptor (PR) isoform expression, nuclear positioning and coregulator expression. Nucl Recept Signal 7: e009. [PubMed: 20087430]

Shyamala G, Yang X, Cardiff RD, Dale E. 2000 Impact of progesterone receptor on cell-fate decisions during mammary gland development. Proc Natl Acad Sci U S A 97: 3044–3049. [PubMed: 10737785]

Shyamala G, Yang X, Silberstein G, Barcellos-Hoff MH, Dale E. 1998 Transgenic mice carrying an imbalance in the native ratio of A to B forms of progesterone receptor exhibit developmental abnormalities in mammary glands. Proc Natl Acad Sci U S A 95: 696–701. [PubMed: 9435255]

Soyal SM, Mukherjee A, Lee KY, Li J, Li H, DeMayo FJ, Lydon JP. 2005 Cre-mediated recombination in cell lineages that express the progesterone receptor. Genesis 41: 58–66. [PubMed: 15682389]

Szwarc MM, Kommagani R, Jeong JW, Wu SP, Tsai SY, Tsai MJ, O'Malley BW, DeMayo FJ, Lydon JP. 2014 Perturbing the cellular levels of steroid receptor coactivator-2 impairs murine endometrial function. PLoS One 9: e98664. [PubMed: 24905738]

Szwarc MM, Kommagani R, Peavey MC, Hai L, Lonard DM, Lydon JP. 2017 A bioluminescence reporter mouse that monitors expression of constitutively active beta-catenin. PLoS One 12: e0173014. [PubMed: 28253313]

Takimoto GS, Tung L, Abdel-Hafiz H, Abel MG, Sartorius CA, Richer JK, Jacobsen BM, Bain DL, Horwitz KB. 2003 Functional properties of the N-terminal region of progesterone receptors and their mechanistic relationship to structure. J Steroid Biochem Mol Biol 85: 209–219. [PubMed: 12943706]

Tan H, Yi L, Rote NS, Hurd WW, Mesiano S. 2012 Progesterone receptor-A and -B have opposite effects on proinflammatory gene expression in human myometrial cells: implications for progesterone actions in human pregnancy and parturition. J Clin Endocrinol Metab 97: E719–730. [PubMed: 22419721]

Tsigkou A, Reis FM, Lee MH, Jiang B, Tosti C, Centini G, Shen FR, Chen YG, Petraglia F. 2015 Increased progesterone receptor expression in uterine leiomyoma: correlation with age, number of leiomyomas, and clinical symptoms. Fertil Steril 104: 170–175 e171. [PubMed: 26006736]

Vegeto E, Shahbaz MM, Wen DX, Goldman ME, O'Malley BW, McDonnell DP. 1993 Human progesterone receptor A form is a cell- and promoter-specific repressor of human progesterone receptor B function. Mol Endocrinol 7: 1244–1255. [PubMed: 8264658]

Wagner KU, Wall RJ, St-Onge L, Gruss P, Wynshaw-Boris A, Garrett L, Li M, Furth PA, Hennighausen L. 1997 Cre-mediated gene deletion in the mammary gland. Nucleic Acids Res 25: 4323–4330. [PubMed: 9336464]

Wardell SE, Boonyaratanakornkit V, Adelman JS, Aronheim A, Edwards DP. 2002 Jun dimerization protein 2 functions as a progesterone receptor N-terminal domain coactivator. Mol Cell Biol 22: 5451–5466. [PubMed: 12101239]

Wetendorf M, Wu SP, Wang X, Creighton CJ, Wang T, Lanz RB, Blok L, Tsai SY, Tsai MJ, Lydon JP, DeMayo FJ. 2017 Decreased epithelial progesterone receptor A at the window of receptivity is required for preparation of the endometrium for embryo attachment. Biol Reprod 96: 313–326. [PubMed: 28203817]

Wu SP, Lee DK, Demayo FJ, Tsai SY, Tsai MJ. 2010 Generation of ES cells for conditional expression of nuclear receptors and coregulators in vivo. Mol Endocrinol 24: 1297–1304. [PubMed: 20382891]

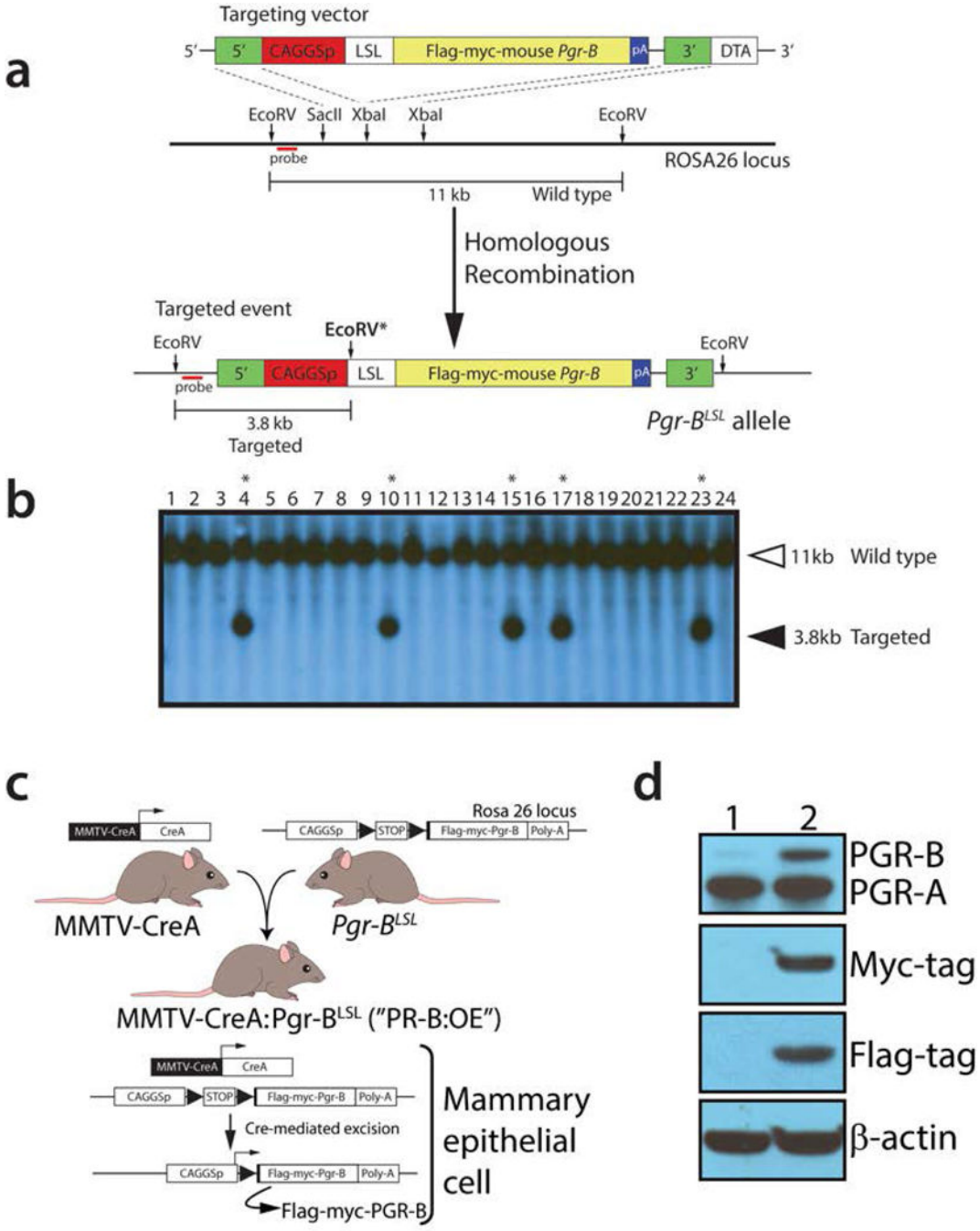

FIGURE 1.

Generation of the *Pgr-B*^{LSL} mouse. (a) Schematic (not to scale) of the targeting strategy in AB2.2 ES cells to generate the *Pgr-B*^{LSL} allele in the *Rosa26* locus. The location of the probe used for Southern analysis of targeted events is shown in red. With EcoRV digestion, the wild type allele is predicted to yield a 11kb hybridization band using this probe. Following homologous recombination with the targeting vector, a positive targeted event is predicated to display a 3.8kb hybridizing band due to an additional EcoRV site (**EcoRV***) within the targeting vector (Wu *et al.*, 2010). The 5' and 3' homology arms of the targeting

vector are indicated in green. The constitutively active promoter is CAGGSp; LSL denotes the LoxP-STOP-LoxP cassette. The epitope-tagged murine Pgr-B cDNA insert is shown in yellow with its strong polyadenylation signal in blue. The targeting vector also contains the diphtheria toxin A gene for negative selection, which was not used in these studies. (b) Typical Southern result using the targeting strategy detailed in (a) above. Lanes 4, 10, 15, 17, and 23 represent positive targeted ES cell clones. Mouse lines were generated from ES cell clones: 4, 10, and 17; mice derived from ES cell clone 17 were analyzed in these studies. (c) Breeding strategy to generate the PR-B:OE by crossing the *MMTV-CREA* transgenic with mice harboring the *Pgr-B*^{LSL} targeted allele. (d) Western analysis of mammary epithelial cell protein isolates derived from virgin control (lane 1) and PR-B:OE (lane 2) mice using primary antibodies against PGR, the myc-tag, and FLAG-tag; β-actin served as a loading control.

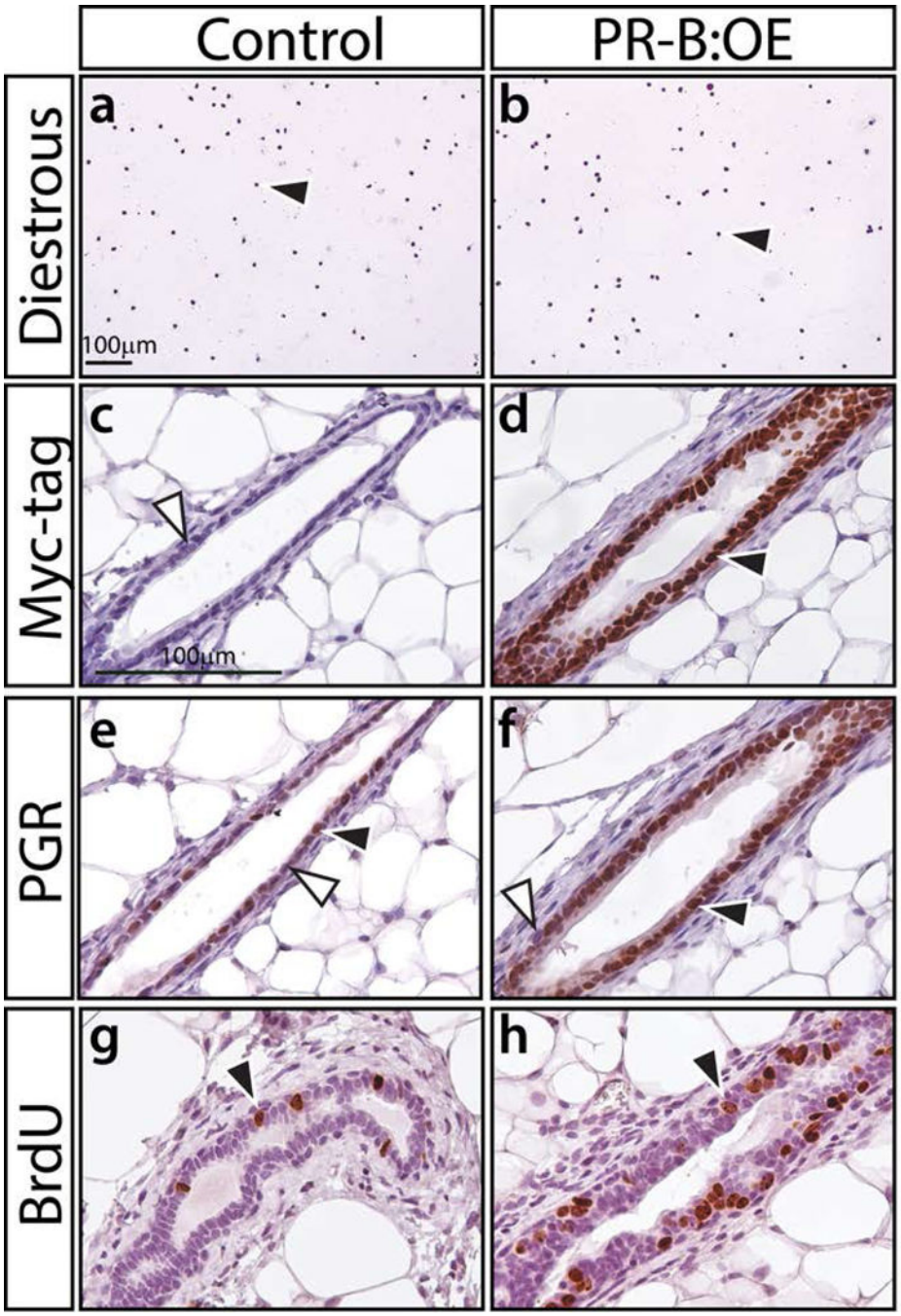

FIGURE 2.

The PGR-B isoform is specifically targeted to the mammary epithelium of the PR-B:OE mouse. (a) and (b) show crystal violet stained vaginal cytology from 8-week old control and PR-B:OE virgin mice respectively. Both genotypes were in diestrus at the time of euthanasia; black arrowhead indicates the presence of leucocytes, which are indicative of the diestrus stage of the estrous cycle. (c) and (d) show a transverse section of a mammary gland duct from control and PR-B:OE mice respectively, which has been stained for myc-tag immunopositivity. Note the expected absence of positive staining in the control gland (white

arrowhead) whereas the PR-B:OE mammary gland duct shows strong staining for the myc-epitope (black arrowhead), which is localized to the epithelial compartment of the mammary duct. (e) and (f) display mammary ducts from control and PR-B:OE mice stained for PGR expression respectively. Note control mammary gland duct shows the typical punctate spatial pattern for PGR expression within the epithelial compartment (positive and negative staining indicated by black and white arrowheads respectively). In contrast, the PR-B:OE mammary gland duct shows stronger PGR staining for the majority of the mammary epithelial cells. (g) and (h) show typical BrdU staining results for the control and PR-B:OE mammary gland respectively at diestrus. Note a significant increase in the number of epithelial cells that score positive for BrdU incorporation (black arrowhead) in the PR-B:OE gland compared to the control gland.

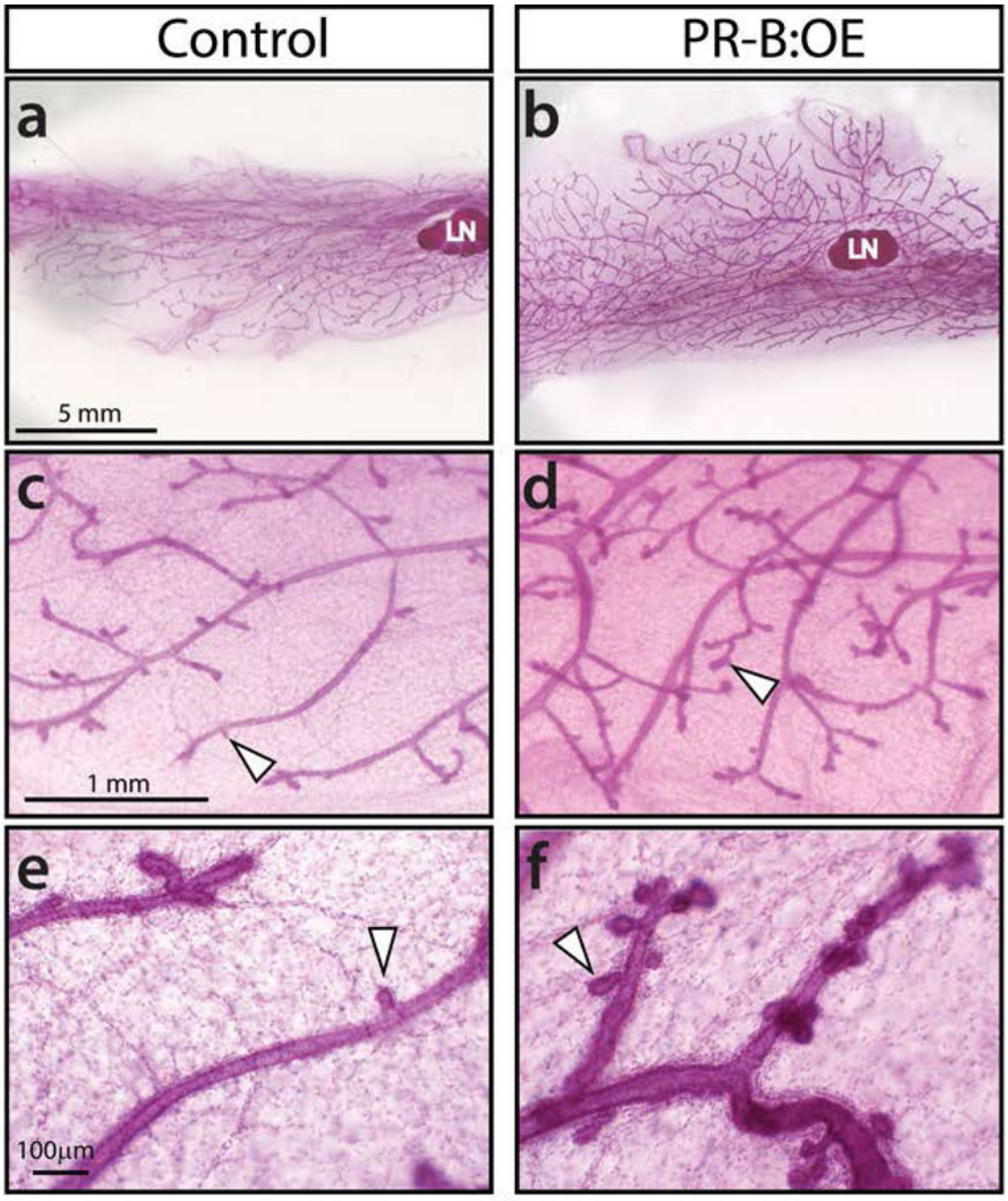

FIGURE 3.

The mammary gland of the virgin PR-B:OE bigenic exhibits an increased number of nascent alveolar buds compared to sibling control glands at diestrus. (a) and (b) show whole mounts of control and PR-B:OE inguinal mammary glands respectively; LN denotes lymph node (a structural reference marker). (c) and (d) are higher magnifications of specific regions shown in (a) and (b) respectively. Note that the structural complexity of the ductal network is markedly increased in the PR-B:OE mammary gland (d) compared to the control gland (c). White arrowheads indicate the location of nascent alveolar buds. (e) and (f) show higher

magnifications of representative ductal regions in the control and PR-B:OE mammary gland respectively. Note the marked increased number of alveolar buds (white arrowheads) in the PR-B:OE mammary gland (f) compared to control (e). Scale bar in (a), (c), and (e) apply to (b), (d) and (f) respectively.

a

Dam genotype	N	# pups born	Average # pups per litter	# pups survive lactation day 2
Control	9	72	8	72
PR-B:OE	16	167	10	0

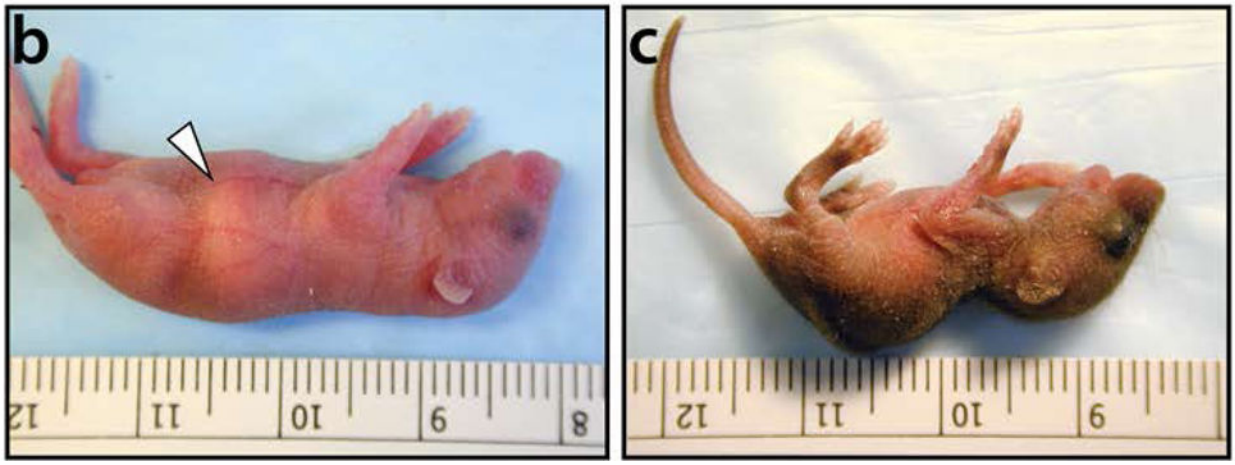

FIGURE 4.

The PR-B:OE dam fails to produce viable litters. (a) Table displays the number (#) of pups that survive two days after birth from control (n=9) and PR-B:OE (n=16) dams. All pups fail to survive from PR-B:OE dams following two days after birth. (b) Image of a typical pup (2-days old) from a control dam, which displays the typical milk band in the stomach region (white arrowhead). (c) Image shows an age-matched monogenic control pup from a PR-B:OE dam. Note the absence of a typical milk band in the stomach region of the pup from the PR-B:OE dam and the pup's overall physical deterioration and diminished size.

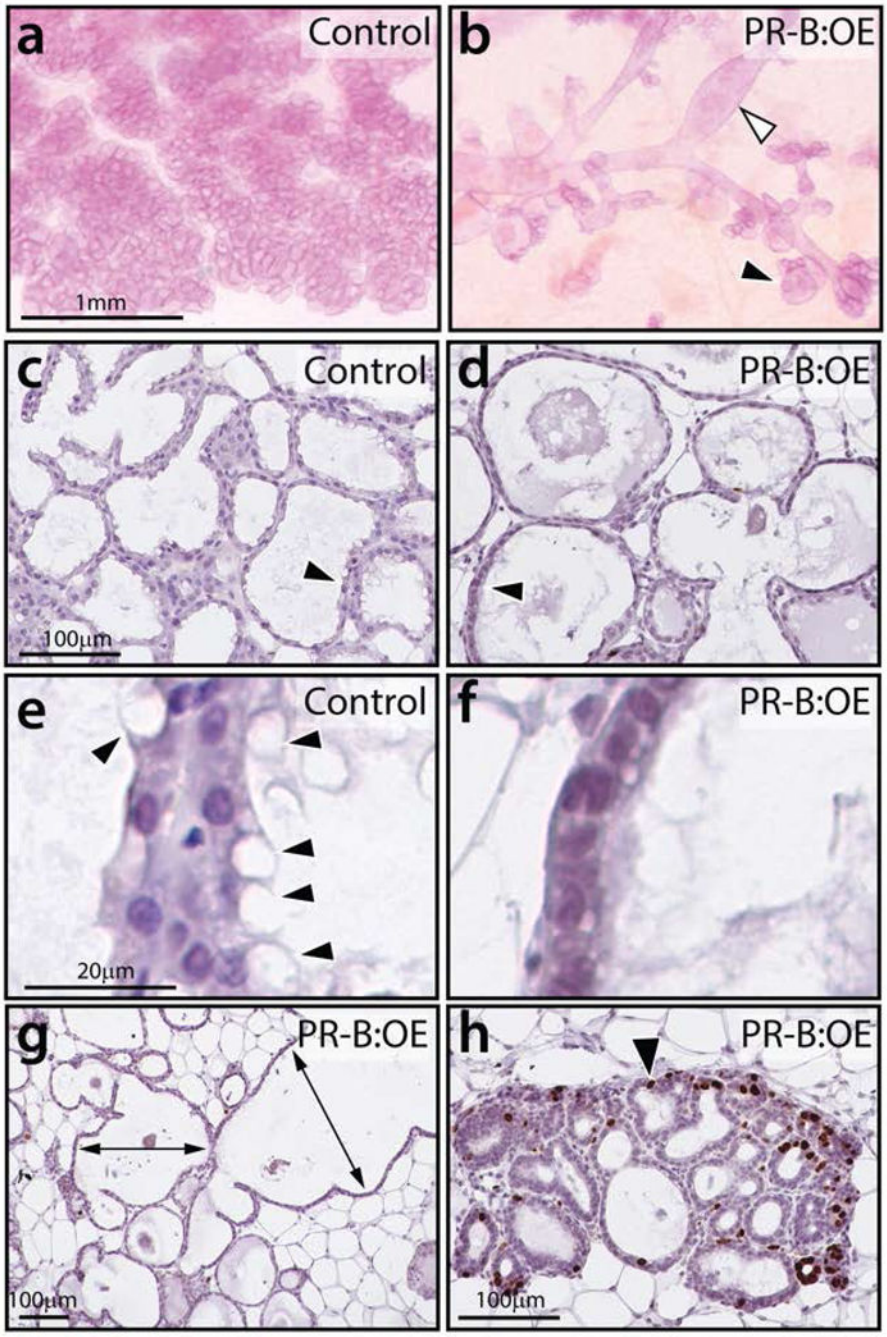

FIGURE 5.

The PR-B:OE mammary gland exhibits an aberrant morphology at lactation. (a) Control mammary gland displays the typical lobuloalveolar structures that completely in-fill the mammary fat pad. (b) The PR-B:OE mammary gland fails to exhibit normal lobuloalveolar morphogenesis. Instead, the PR-B:OE mammary gland shows aberrant dilated ducts (white arrowhead) with abnormal alveolar budding (black arrowhead). (c) Transverse section of lobuloalveolar structures in control mammary gland that are stained for BrdU incorporation. Note the absence of cells scoring positive for BrdU. (d) Transverse section of corresponding

PR-B:OE mammary gland, note the overtly distended epithelial ducts (arrowhead). (e) Higher magnification of (c) shows the presence of numerous vacuolated epithelial cells with lipid droplets (arrowheads). (f) Higher magnification of (d) showing the absence of these vacuolated epithelial cells in the PR-OE mammary gland. (g) A low magnification image of the PR-B:OE mammary gland stained for BrdU incorporation. While large areas of the gland do not show regions of proliferation, the PR-B:OE mammary tissue is clearly abnormal with extreme ductal dilation (double headed arrows). (h) shows areas in the PR-B:OE tissue that exhibit foci of epithelial cells with numerous cells scoring positive for BrdU incorporation (black arrowhead). Scale bar in a; c; and e applies to b; d; and f respectively.

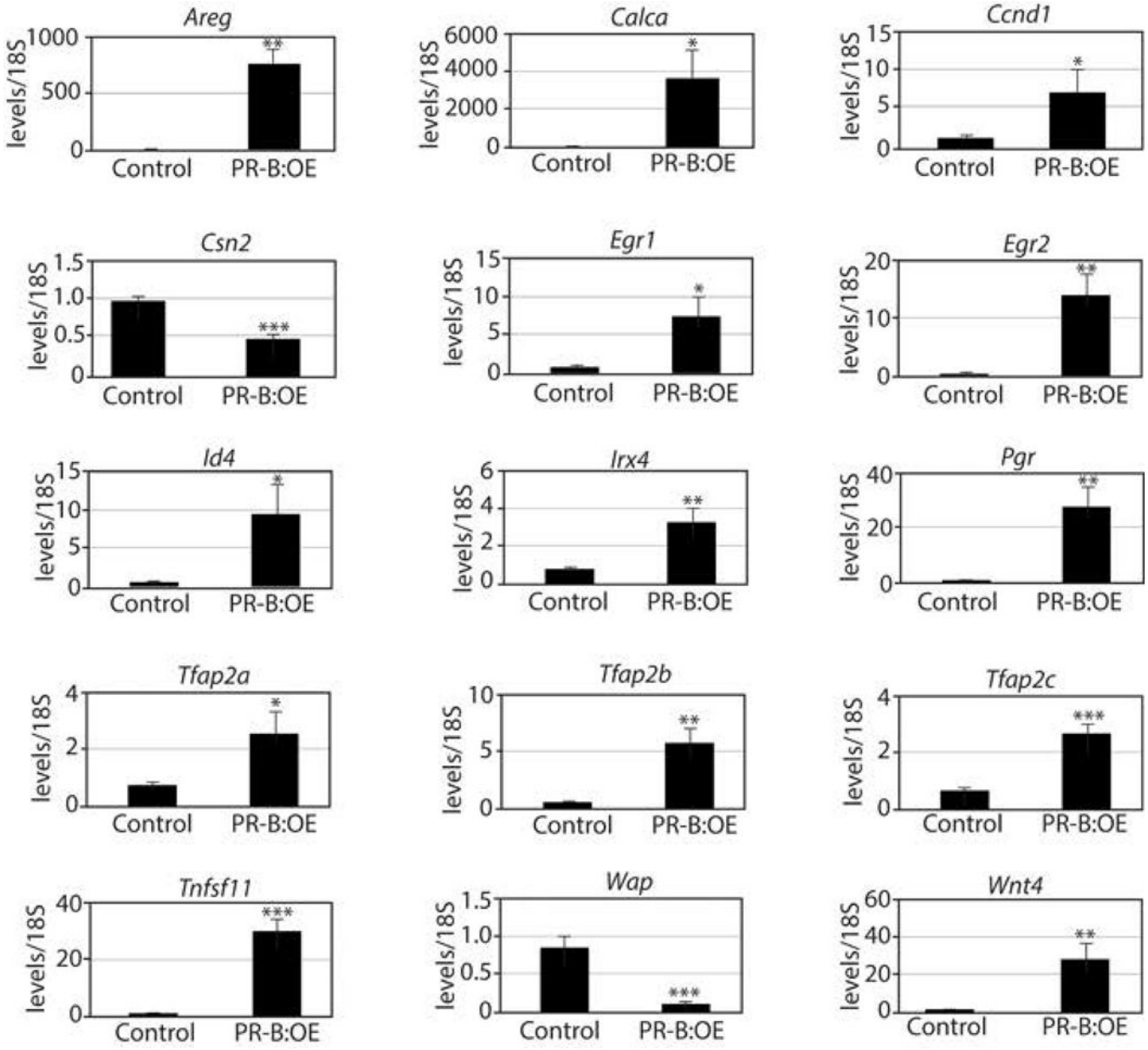

FIGURE 6.

Aberrant transcriptional programming in the PR-B:OE mammary gland. Histograms display quantitative real time PCR results of the relative transcript levels of PGR target genes as well as genes indicative of the normal terminally differentiated mammary gland at lactation. Note the expression levels of markers of mammary gland differentiation are significantly reduced in the PR-B:OE mammary gland (two-days post-parturition) compared to the corresponding control whereas PGR targets are abnormally elevated in the PR-B:OE mammary gland compared to control.